Comparison and Combination of NLPQL and MOGA Algorithms for a Marine Medium-Speed Diesel Engine Optimisation

Nao Hu[1, 2,*], Peilin Zhou[1], Jianguo Yang[2, 3]

(*1. Department of Naval Architecture and Marine Engineering, University of Strathclyde, G4 0LZ, Glasgow, UK;*

2. School of Energy and Power Engineering, Wuhan University of Technology, 430063, Wuhan, PRC;

3. Key Laboratory of Marine Power Engineering &Technology, Ministry of Communications, 430063, Wuhan, PRC;

**. Corresponding author*)

Abstract: Seven engine design parameters were investigated by use of NLPQL algorithm and MOGA separately and together. Detailed comparisons were made on NOx, soot, SFOC, and also on the design parameters. Results indicate that NLPQL algorithm failed to approach optimal designs while MOGA offered more and better feasible Pareto designs. Then, an optimal design obtained by MOGA which has the trade-off between NOx and soot was set as the starting point of NLPQL algorithm. In this situation, an even better design with lower NOx and soot was approached. Combustion processes of the optimal designs were also disclosed and compared in detail. Late injection and small swirl were reckoned to be the main reasons for reducing NOx. In the end, RSM contour maps were applied in order to gain a better understanding of the sensitivity of import parameters on NOx, soot and SFOC.

Keywords: comparison; combination; NLPQL; MOGA; RSM

Nomenclature

ATDC	after top dead centre	Soot_b	soot emission of baseline design
BTDC	before top dead centre	Soot_M	the design of minimum soot emissions with MOGA
CFD	computational fluid dynamics	Soot_N	the design of minimum soot emissions with NLPQL method
CO	carbon monoxide	SQP	sequential quadratic programming
CO2	carbon dioxide	SR	swirl ratio

* Corresponding author.

Email address: nao.hu.0128@gmail.com (N. Hu).

d003	connection length	SS-ANOVA	smoothing spline analysis of variance
DI	direct injection	TDC	top dead centre
DoE	design of experiment	μGA	micro-genetic algorithm
Dukowicz	fuel oil spray model	v001	the distance from the centre of toroidal surface to the piston top surface
GA	genetic algorithm	v002	clearance
h001	bowl radius	v003	crown centre height
HC	hydrocarbons	Walljet1	wall interaction model
KIVA	a Fortran-based CFD software	Zeldovich	NOx emission model
k-zeta-f	turbulence model		
L100	full engine load		
L25	25% engine load	Functions and variables	
L50	50% engine load	x	n-dimensional parameter vector
L75	75% engine load	μ_i	weight
LDC	lower dead centre	E	set
LDO	light diesel oil	f	function
LMA	Levenberg-Marquardt algorithm	g_j	function
Max	maximum	j	variable
Min	minimum	k	objective
MOGA	multi-objective genetic algorithm	m	maximum value of j
NLPQL	non-linear programming by quadratic Lagrangian	m_e	real number
NN	neural networks	N	maximum objective numbers
NOx	nitrogen oxides	O_i	objectives of merit function
NOx_b	NOx emissions of base-line design	R^n	n-dimensional real space
NOx_M	the design of minimum NOx emissions with MOGA	$\vec{x}^*$	Pareto design
NOx_N	the design of minimum NOx emissions with NLPQL method	$\vec{x}_j$	arbitrary design
NPL	nozzle protrusion length	x_Q	lower bound of x
NSGA II	non-dominated sorting genetic algorithm II	x_u	upper bound of x
OPT_M	the design with best balance of MOGA		
OPT_M&N	the best design of combined method	Units	
OPT_N	the best design of NLPQL algorithm	℃	degree Celsius
Piso	pressure implicit split operator	CA	crank angle
r002	toroidal radius	deg	degree
RSM	response surface methodology	g/kWh	grams per kilowatt-hour
SA	spray angle	L	litre
SFOC	specific fuel oil consumption	k	kilo

SFOC_b	specific fuel oil consumption of baseline design	kW	kilo Watt
SFOC_M	the design of minimum SFOC with MOGA	mm	millimetre
SFOC_N	the design of minimum SFOC with NLPQL	mm^2/s	square millimetre per second
Simple	semi-implicit method for pressure linked equations	r/min	rotates per minutes
Sobol	quasi-random low-discrepancy sequences	% (mass)	percent by mass
SOI	start of injection	% (volume)	percent by volume

1 Introduction

Marine diesel engines play an indispensable role in ships, however, the intolerable pollution caused by them gains increasing attentions around the world. Comparing to automotive diesel engines, CO, CO2 and HC emissions generated by marine diesel engines are much lower, whereas NOx emissions are severely deteriorated. Although after-treatment devices are effective in reducing emissions, the optimisation of engine combustion is still of great significance. However, combustion is very susceptible to the match status of the fuel injector and combustion chamber. A lot of meaningful work has been done on this subject, Taghavifar et al. [1] studied the effects of bowl movements and radius on mixture formation in terms of homogeneity factor, combustion initiation and emissions for a 1.8 L Ford diesel engine. They pointed out the mixture uniformity increased as the bowl displacement toward the cylinder wall, but got penalty of a rise of combustion delay which substantially reduces the effective in-cylinder pressure. They also found that smaller bowl size contributes to better squish and vortex formation in the chamber, although with lesser spray penetration and flame quenching. Park [2] used a micro-genetic algorithm coupling with a KIVA code to optimise combustion chamber geometries and engine operating conditions for an engine fuelled with dimethyl ether. He found the combustion and emission characteristics were significantly different from that of conventional diesel engines. Mobasheri et al. [3] investigated the influence of a re-entrant

combustion chamber geometry on mixture forming, combustion and performance for a high-speed direct injection diesel engine. Thirteen combustion chambers with different shapes were designed by adjusting piston parameters, i.e. bowl depth, bowl width, piston bottom surface and the lip area. Results indicated that small bowl diameter is the main reason for high soot emissions, and a slightly larger bowl diameter is where the optimal operating point locates.

Recently, the ever-changing calculation ability of computers brings the computational fluid dynamics to a more sophisticated and precise level. Some algorithms were frequently used in engine optimisation domain. High efficiency was achieved in the study of a huge amount of optimisation cases. Researchers of references [4-7] developed a KIVA code with μGA, MOGA or NSGA II to study the matching of a variety of engine parameters. From small bore high-speed direct injection engines to heavy-duty large bore slow-speed diesel engines. This huge amount of optimisation work was done owing to the effective optimisation algorithms[4, 5, 6, 7]. Taghavifar et al. [8] used a DoE method incorporating with a Sobol sequence to scan through various design points of a 1.8 L Ford diesel engine, aimed to seek a reduction of NOx and an enhancement of the spraying performance. He found the optimal case has a lower injection angle and a smaller bowl volume. Jeong et al. [9] used a hybrid evolutionary algorithm by coupling a GA and a PSO for the optimisation of a diesel combustion chamber. Results indicated that hybrid evolutionary algorithm shows better diversity and convergence. Chen et al. [10] used an orthogonal design method to optimise the match of injection-related parameters with three combustion chamber geometries for an 8.9L Cummins diesel engine. Then, NLPQL algorithm was adopted for a more detailed study on combustion chamber geometries.

Some meaningful work on the comparisons of these algorithms used for engine optimisation were also investigated. Shi et al. [11] assessed μGA, NSGA II and ARMOGA incorporating

with a KIVA code for the optimisation of combustion chamber under the same conditions. Results indicated that the NSGA II algorithm with a large population of 32 performed the best by considering the optimal solutions' optimality and diversity. Navid et al. [12] compared GA and NLPQL algorithms when they were used for the optimisation of a Ford 1.8L DI engine. Four factors including injection angle, half spray cone angle, inner distance of bowl wall and bowl radius were selected to be optimised. Results showed that NLPQL approaches an optimal design faster than GA. It would be interesting to know whether NLPQL algorithm would still be efficiency when it is introduced for the optimisation of seven engine design parameters of a marine medium-speed diesel engine.

In principle, the NLPQL algorithm is a local optimisation algorithm. Whether an optimal design can be reached or not relies heavily on the starting point, because once the NLPQL algorithm reaches a local optimum, there is no mechanism to get away from it [13]. So a good starting point is crucial for the NLPQL algorithm. However, MOGA is a global algorithm that a starting point is of no effect. A better method is that the optimal design achieved by MOGA is set as the starting point of NLPQL algorithm. To the best knowledge of the author, this kind of study was never seen in the optimisation of a marine medium-speed diesel engine with seven design parameters.

RSM was frequently used as the tool for analysing the sensitivity of design parameters on the NOx, soot and SFOC [6, 14]. It uses an approximation model to analyse the data generated by Design of Experiments (DOE). Several functions can be used for building approximation models, such as polynomials, smoothing spline ANOVA, NN [15, 16, 17], etc. Comparisons were made in literature and the NN were recommended for having a better accuracy and performance in the prediction process [18, 19, 20].

In this paper, NOx, soot and SFOC are the three sub-objectives to be optimised. NLPQL algorithm and MOGA were compared for the optimisation of seven match parameters of injector and combustion chamber for a marine medium-speed diesel engine. The seven parameters including injection timing, spray angle, nozzle protrusion length, swirl ratio, bowl diameter, centre crown height and toroid radius. Then, the optimal design of MOGA was set as the starting point of the NLPQL algorithm for seeking a possible better optimum. Finally, the influences of design parameters on objectives were discussed by RSM.

2 Algorithms

2.1 NLPQL algorithm

NLPQL was developed by Klaus Schittkowski [21] for solving the nonlinear programming problem.

$$\min f(\mathrm{x}) \quad \begin{matrix} g_j = 0, j = 1,...,m_e \\ x \in R^n : g_j(x) \geq 0, j = m_e + 1,...,m \\ x_Q \leq x \leq x_u \end{matrix} \tag{1}$$

Where, x is the n-dimensional parameter vector. x_Q and x_u are the lower bound and upper bound of x. $f(\mathrm{x})$ is the problem function. $g_j(x)$ are the constraints of the problem.

The optimisation method generates a sequence of quadratic programming subproblems which are to be solved successively. The method is therefore known as the SQP method. It assumes that objective functions and constraints are continuously differentiable on the set $E = \{x \in \Re^n : x_Q \leq x \leq x_u\}$. Note that the functions f and $g_j, j = 1,...,m$ need to be defined only

in the set *E*, since the iterations computed by the algorithm will never violate the lower and upper bounds.

If NLPQL algorithm is used to solve a multi-objective problem, a merit function with a weighted sum method must be adopted to transfer it to a single objective optimisation problem. The formula of weight sum method is

$$Objective = \sum_{i=1}^{k} \mu_i O_i(x) \tag{2}$$

In(2), μ_i is the weight of each objective, which is decided by researchers according to their experiences, O_i are the objectives.

In this paper, the merit function is built in(3) to reduce the NOx and Soot emissions, and minimise the fuel consumption rate as well. The weights are given according to experience and literature [10].

$$\text{Objective} = \left(\frac{NOx}{NOx\_b}\right)*5 + \left(\frac{Soot}{Soot\_b}\right)*1 + \left(\frac{SFOC}{SFOC\_b}\right)*3 \tag{3}$$

Where, NOx_b, $Soot\_b$, $SFOC\_b$ are the values of baseline design.

2.2 MOGA

The GA is based on the idea of natural selection which obeys the law of 'survival of fittest'. It can continually improve the average fitness level of a population by means of inheritance, mutation, selection and crossover, eventually leading to an optimum design [22]. MOGA is the modification version of GA in order to find a set of multiple non-dominated solutions in a single run [23].

2.3 Pareto optimum

Pareto optimum is often adopted in multi-objective occasions, as shown in Fig. 1. Case A-D can be considered as Pareto optimal cases due to the fact that none of them is out-performed by other cases. These cases can be grouped together as a Pareto front. The Pareto optimality can be defined as: For all designs and the corresponding N objectives $f_k(\vec{x})$, where, k= 1, 2, …, N, the Pareto design $\vec{x}$ is defined as the following: for an arbitrary design j, there exists at least one objective, k, meets the condition $f_k(\vec{x}_j) \succ f_k(\vec{x})$. MOGA's mission is to find the Pareto optimums while keeping diversity in the results [6].

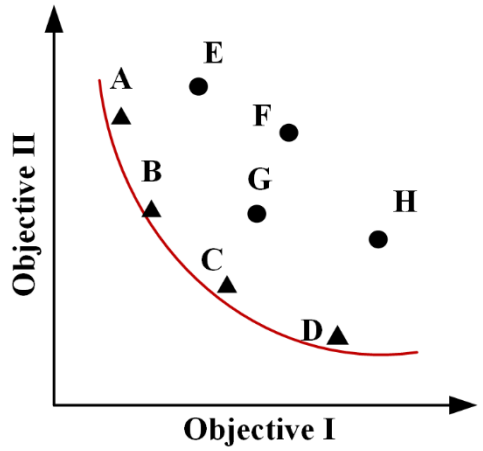

Fig. 1 Definition of Pareto optimums

2.4 Neural networks

Neural networks are based on the idea of imitating the structure of information process in human brains. They are made up of fundamental computing units and perceptrons, which are assembled to form a network. Neural networks are suitable for nonlinear problems by introducing nonlinear transformations to the flow of information between the layers of perceptrons [24].

The neural networks used here is a classical feedforward one, with one hidden layer and an efficient Levenberg-Marquardt back propagation training algorithm. Levenberg-Marquardt algorithm (LMA) is popular for neural networks training. It was independently developed by Kenneth Levenberg and Donald Marquardt [25, 26]. It solves a problem by minimizing a non-linear function with fast speed and stable convergence.

3 Preparation

3.1 Engine specification

The main specifications of the marine medium-speed diesel engine and fuel injectors are presented in Table 1. It is an in-line type four stroke diesel engine with six cylinders. Its rated speed and rated powers are 1000 rpm and 540 kW respectively. The spray orifice distribution of original injector of mechanical fuel injection system is 9*0.28 mm, which is replaced by an electronic fuel injector of 9*0.23 mm for the performance and emission prediction study.

Table 1 Specifications of the engine and fuel injectors

Specifications	Value
Engine name	MAN 6L16/24
Cylinder arrangement	In-line
Number of stroke	4
Bore(mm)	160
Stroke(mm)	240
Number of cylinders	6
Rated speed (r/min)	1000
Rated power (kW)	540

SFOC (g/kWh)	189
Compression ratio	15.2
Original injector	9*0.28 mm
Electronic fuel injector	9*0.23 mm

164

165 **3.2 Simulation model**

166 Simulations were conducted by using a series of AVL FIRE software. Here, the k-zeta-f [27,28]
167 turbulent model for high Reynolds numbers was adopted to describe the flow field inside a
168 combustion chamber. Stand wall function was used to describe heat transfer of wall. Piso
169 algorithm[10, 29, 30] was adopted here to solve the highly unsteady state flow of combustion
170 problem. In terms of fuel spray model, Dukowicz [31] model was applied for handling the heat-
171 up and evaporation of fuel oil droplets. Moreover, Wave [32, 33] break-up model and
172 Walljet1[34, 35] wall interaction model were used respectively. The Eddy break-up model [36,
173 37] was introduced in the calculation of combustion. With regard to emission models, extended
174 Zeldovich [38] was adopted for NOx emission model while Kinetic for soot emission model
175 [39, 40, 41].

176

177 **3.3 Model verification**

178 A FIRE simulation model of the original diesel engine was executed on the condition of rated
179 engine speed and four engine loads. Light diesel fuel oil (represented by DIESEL-D1 in AVL
180 Fire software) is used in the calculation. LDO is a blend of distillate fuel with a small proportion
181 of residual fuel. Thus, a number of properties must meet standard requirements for a fuel to be
182 classified as light diesel oil. The standard requirements were reported in Table 2 [42]. In order
183 to improve the convergence at the beginning of the calculation, the initial calculation step is

184 set to 0.2 CA. Then, 1CA is adopted at compression stroke to accelerate calculation and save
185 time. However, at injection stage, precision is emphasised by reducing calculation step to 0.2
186 CA again. In expansion combustion stage, 0.5 CA is adopted. With regard to average mesh
187 size, Abraham [43] recommended the mesh size to be on the same length scale with nozzle
188 diameter. Thus, the average mesh size is set to 1mm, totally 125k cells were calculated. Fig. 2
189 shows the mesh of original combustion at 0 deg CA (TDC), 64.5 deg CA and 180 deg CA
190 (LDC), which are described by (a), (b) and (c) in Fig. 2 respectively. The mesh at TDC has
191 minimum cell numbers of 4063 while the mesh at LDC has maximum cell numbers of 15833.

192 Table 2 Properties requirements for LDO

Property	Requirements		Units
Cetane number	35-38 (for typical LDO)		_
Pour point, Max	Winter	12	℃
	Summer	18	
Flash point, Pensky-Martens, Min	66		℃
Kinematics viscosity, at 40 ℃	2.5 to 15.7		mm^2/s
Sediment, Max	0.1		% (mass)
Total Sulphur, Max	1.8		% (mass)
Water content, Max	0.25		% (volume)

193

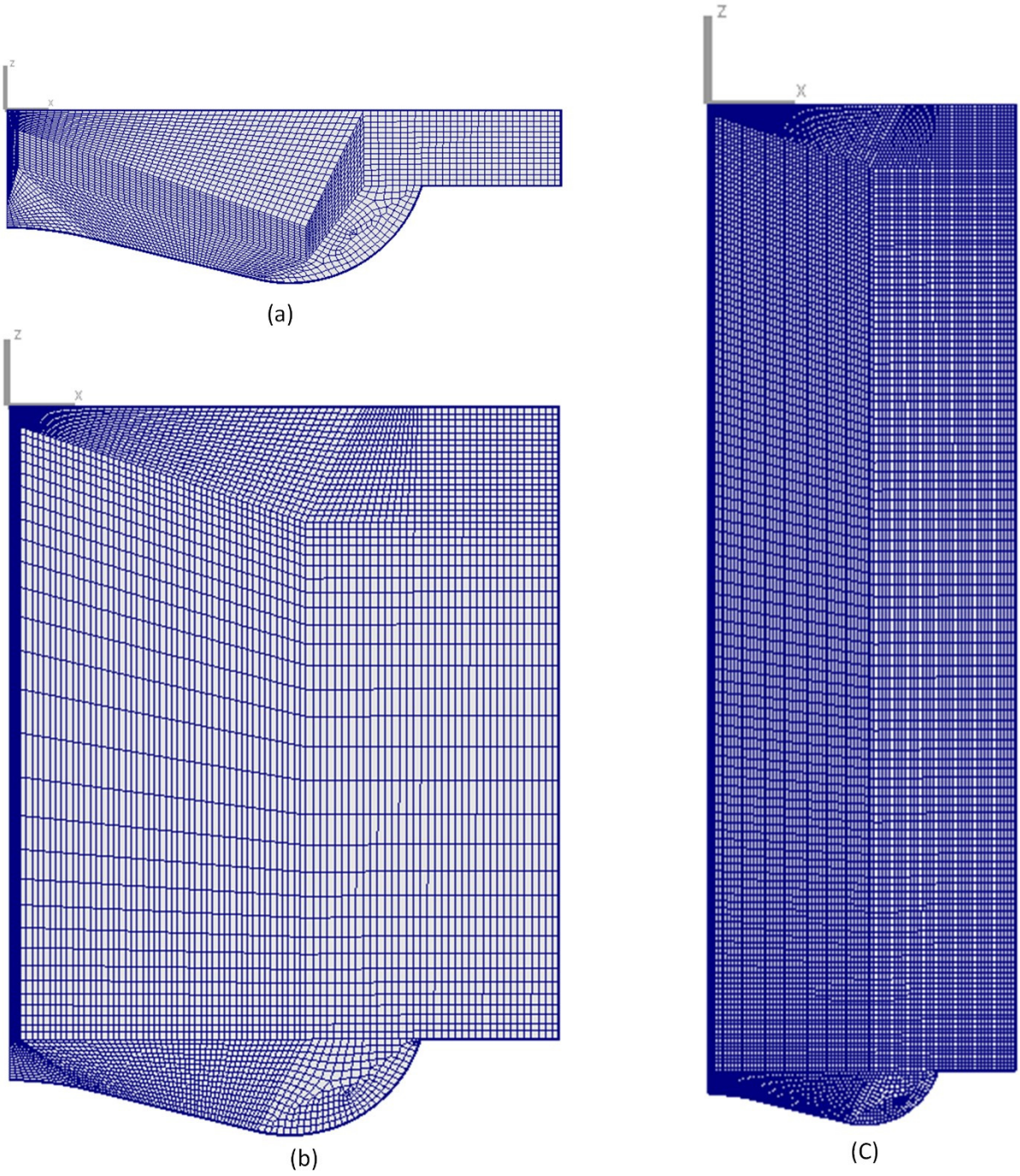

Fig. 2 Mesh changes with piston movements

The comparisons of the cylinder pressures between the simulation data and test data of four loads are shown in Fig. 3. It can be seen that a good agreement of simulation data and experimental data is achieved, especially at the stage of combustion. In the stage of compression and expansion, simulation data were a little bit larger than test data, that's because

the pressure losses by leakage were not considered in this simulation model, while these losses do exist in authentic diesel engines.

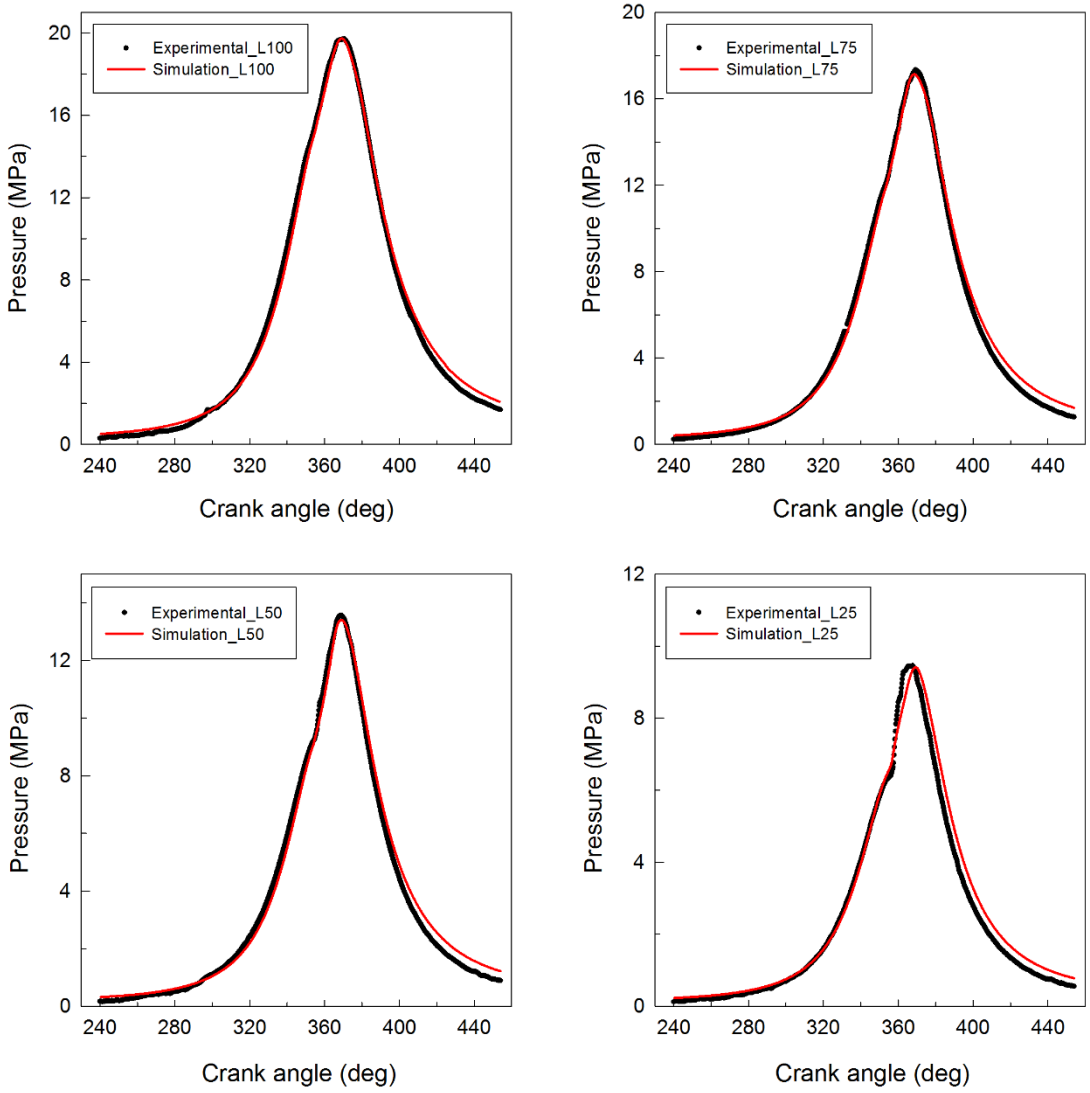

Fig. 3 Pressure comparisons of experimental data and simulation data of four engine loads

NOx emissions are also examined and compared at each engine load. As shown in Fig. 4, the main trend of simulation results corresponds to the experimental data. The maximum error occurred at full load which is less than 6.5%.

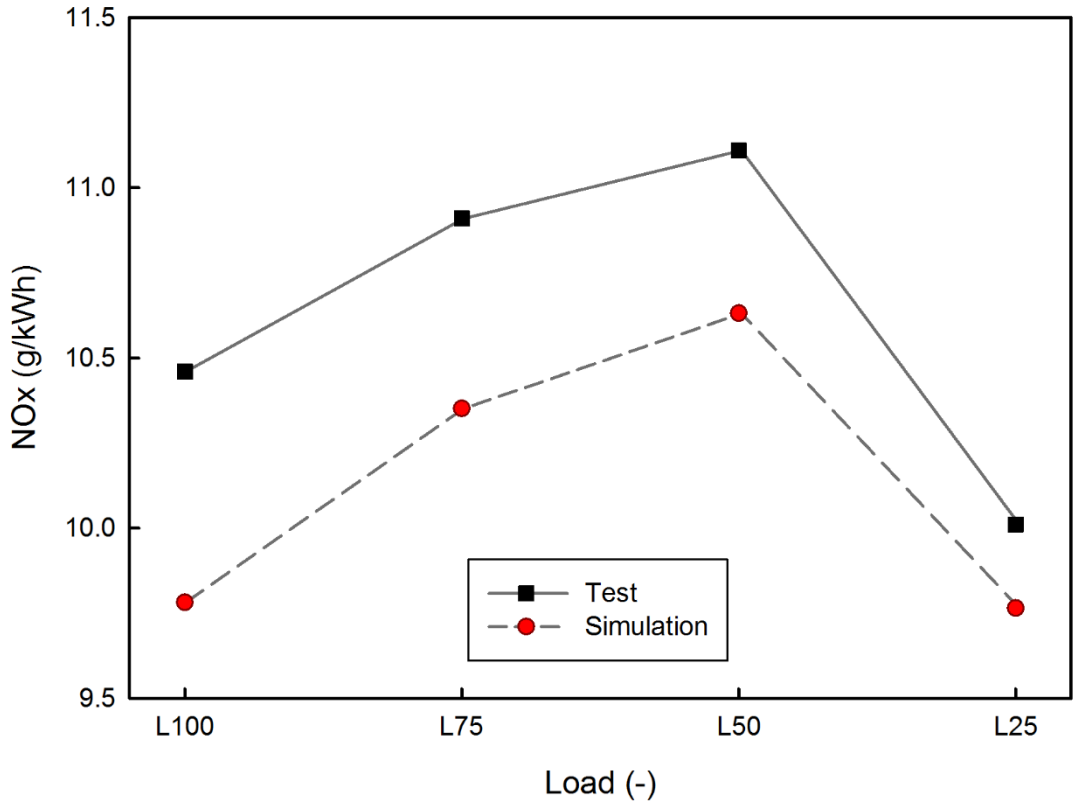

Fig. 4 NOx emission comparison of test data and simulation data of four engine loads

Verification indicates that the model can be used to simulate and predict the engine performance when replacing the original mechanical fuel injection by a high-pressure common rail injection system. The engine body with the high-pressure common rail fuel injection system is defined as the baseline engine, which kept the match parameters the same as the original one.

3.4 Design parameters and variation ranges

Fig. 5 demonstrates the overall shape of the combustion chamber. Bowl diameter is twice of the h001, the toroidal radius is represented by r002 and the centre crown height is represented by v003. Other geometry parameters like v001, v002 and d003 are adjusted automatically in

222 software to keep the compression ratio the same. The variation ranges of the design parameters
223 were shown in Table 3.

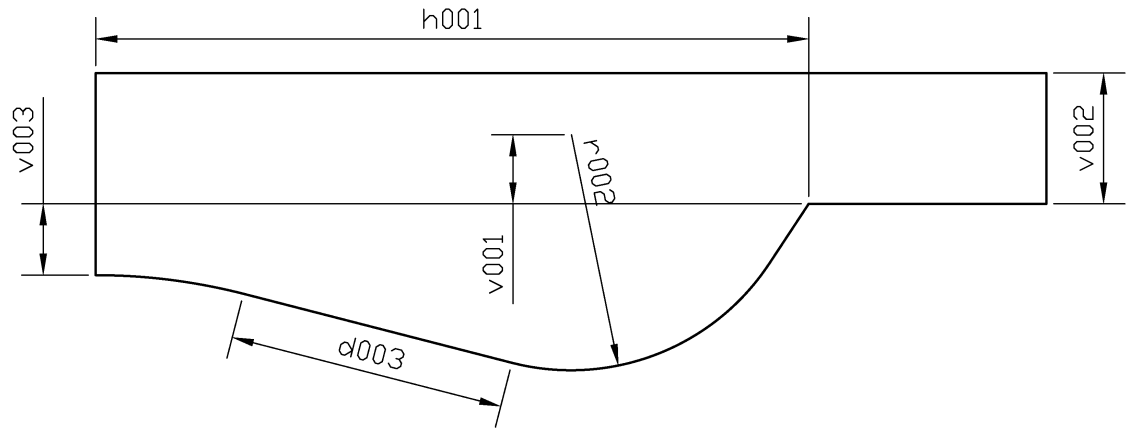

224

225 Fig. 5 Sketch of combustion chamber geometry parameters

226

227 Table 3 Variation ranges of design parameters

Parameters	Code	Baseline	Lower bound	Upper bound
Injection timing, CA	SOI	710	700	720
Swirl ratio, -	SR	1.0	0.5	2.5
Spray angle, deg	SA	143	131	155
Nozzle protrusion length, mm	NPL	2.5	1.0	4.0
Toroidal radius, mm	r002	20	18	22
Centre crown height, mm	v003	6	5	9
Bowl diameter, mm	2*h001	120	108	132

228

229 **3.5 Optimisation settings**

230 The optimisation settings of the NLPQL algorithm are listed in Table 4. Latin hypercube
231 method was used before NLPQL algorithm each time during the optimisation process.

232

Table 4 Optimisation setting of NLQPL algorithm

Property	Value
Maximum number of function evaluations	5
Maximum number of iterations	20
Step size for finite difference step	0.001
Accuracy	1e-05

The optimisation settings of MOGA are listed in Table 5. Distribution for crossover probability and for mutation probability both set as the default value 10. Generation number of 10 and population size of 20 are adopted here. Usually, crossover probability and mutation probability are set to 0.7 and 0.1 respectively.

Table 5 Optimisation setting of MOGA

Property	Value
Distribution for crossover probability	10.0
Distribution for mutation probability	10.0
Number of generations	10
Population size	20
Crossover probability	0.7
Mutation probability	0.1

All of the simulations below were executed under L100 engine load.

4 Comparisons between NLPQL algorithm and MOGA

4.1 Optimisation history comparison

Fig. 6 and Fig. 7 report the optimisation history with NLPQL algorithm and MOGA respectively. The red vertical dash line indicates the Run ID 17 has the minimum objective. The red circle points identify the history of objectives. The ratios of NOx, soot and SFOC to the baseline design are represented by black diamond points, blue triangle points and reversed yellow triangle points respectively.

In Fig. 6, the first 30 results were Latin hypercube designs. The rest runs were the searching history with the NLPQL algorithm. The best objective located at Run 17. The total runs of NLPQL algorithm end at 90. In Fig. 7, the total runs ends at 240. Usually, MOGA optimisation is much more time consuming than NLPQL optimisation.

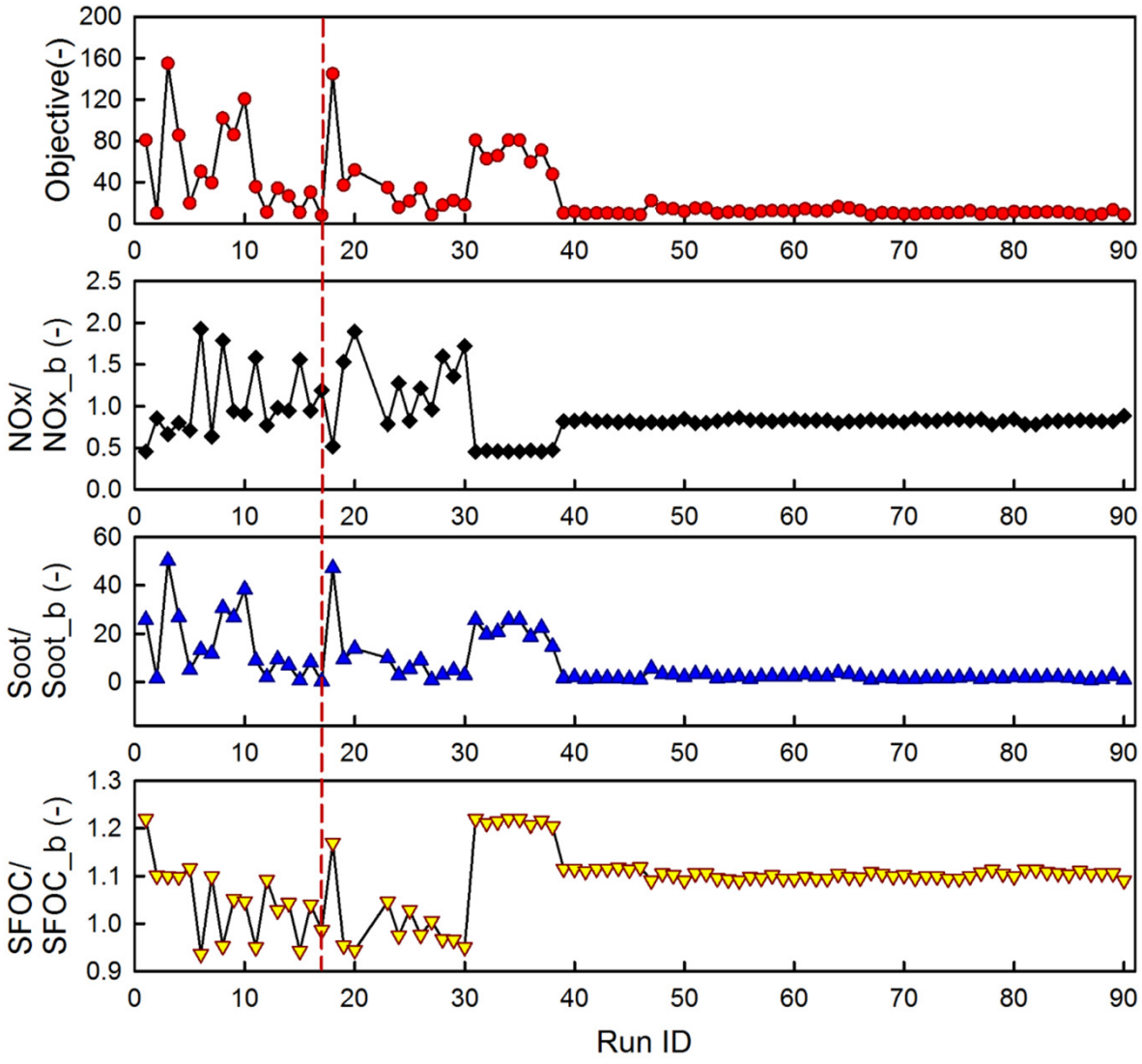

255

256 Fig. 6 Optimisation history with NLPQL algorithm

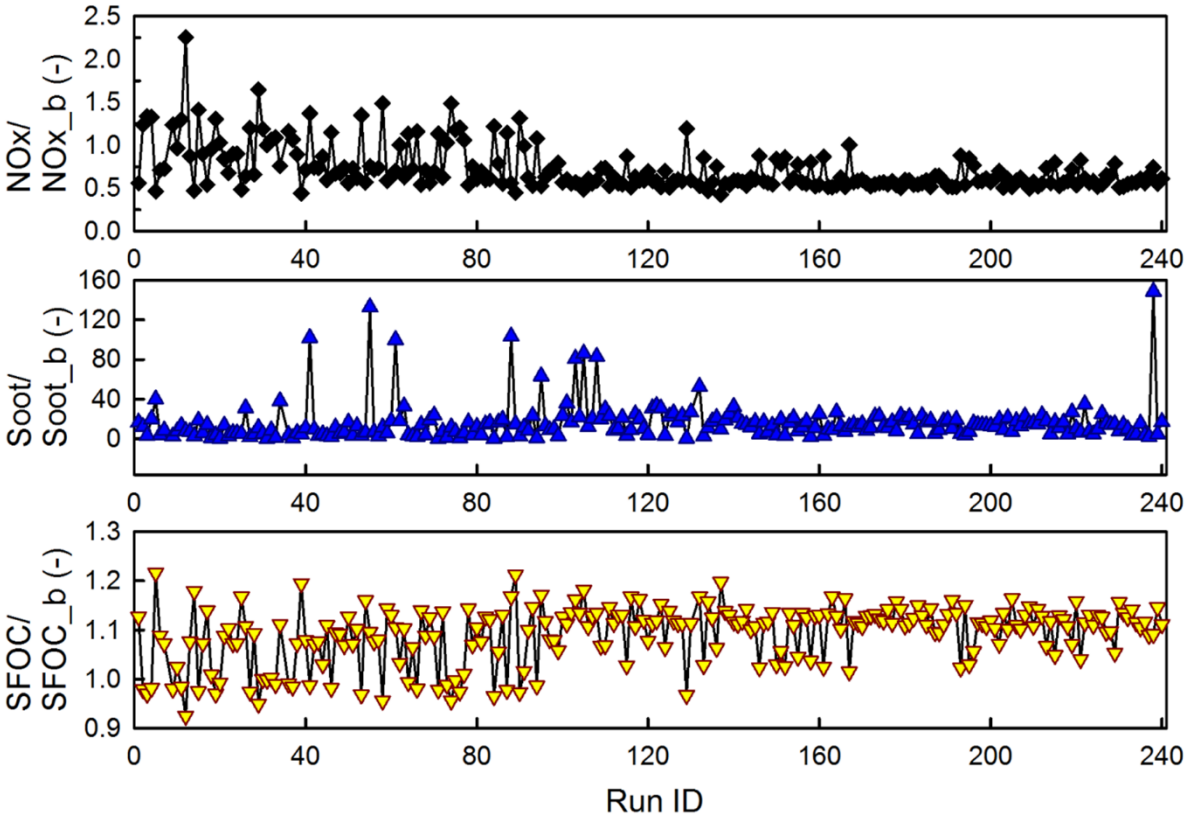

Fig. 7 Optimisation history with MOGA

4.2 Objective comparison

Fig. 8 and Fig. 9 show the scattering maps of NOx vs soot and NOx vs SFOC for NLPQL algorithm and MOGA respectively. The optimal design Run ID 17 yielded by NLPQL algorithm is defined to OPT_N, and also be represented by blue triangle point. The black rectangular points stand for the baseline design and the black hollow triangle points represent Pareto solutions. The OPT_N gained a huge reduction of soot by 94.8% and a slight drop of SFOC by 3.9%. Details were shown in Table 6. The soot emissions for the baseline engine are already ultra-low, thus, further reduction of soot seems to be the icing on the cake. A more prominent issue is to cut down NOx emissions. However, the OPT_N failed to reduce NOx emissions but increased by 18.7% instead. From the scattering maps, there surely exists a better trade-off point between NOx emissions and soot emissions, but the objective function failed to

spot it. This kind of failure maybe linked to the improper chosen of weights in the merit function of NLPQL algorithm.

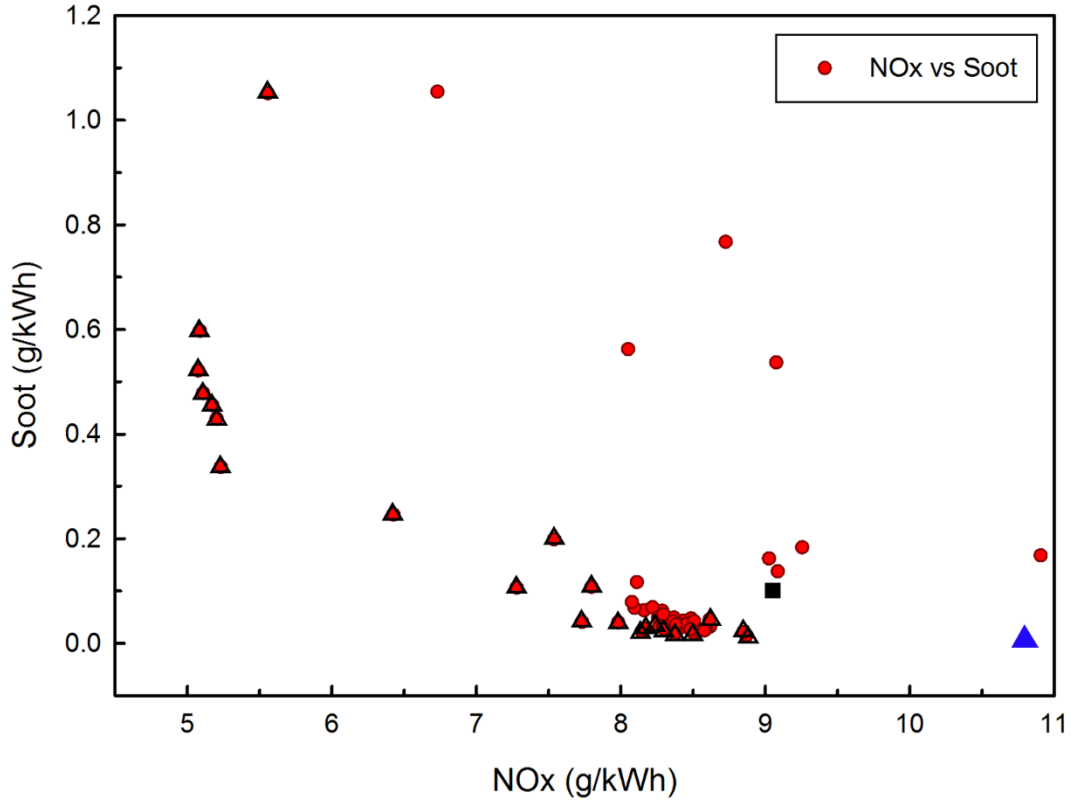

Fig. 8 NOx vs soot of NLPQL algorithm

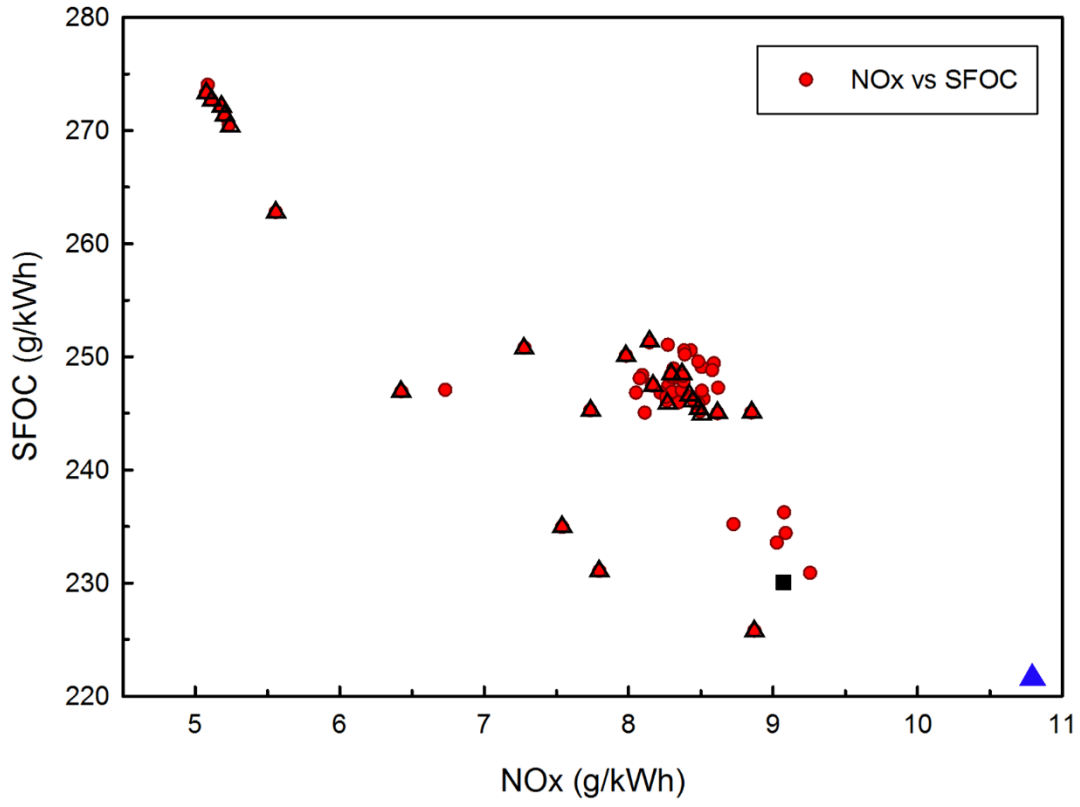

Fig. 9 NOx vs SFOC of NLPQL algorithm

Fig. 10 and Fig. 11 show the optimisation results obtained with MOGA. In the scattering charts, all of the Pareto designs are the feasible solutions for the multi-objective design. The Pareto design with the best trade-off between NOx and soot was selected as the optimal design. Here the optimal design is Run ID 14, which was also represented by OPT_M and marked with a blue diamond point. Comparing to the baseline design, the optimal design achieves a reduction of NOx emissions by approximately 44%, soot emissions by 33%, whereas gets a penalty of SFOC increase by nearly 15%. As shown in Table 6.

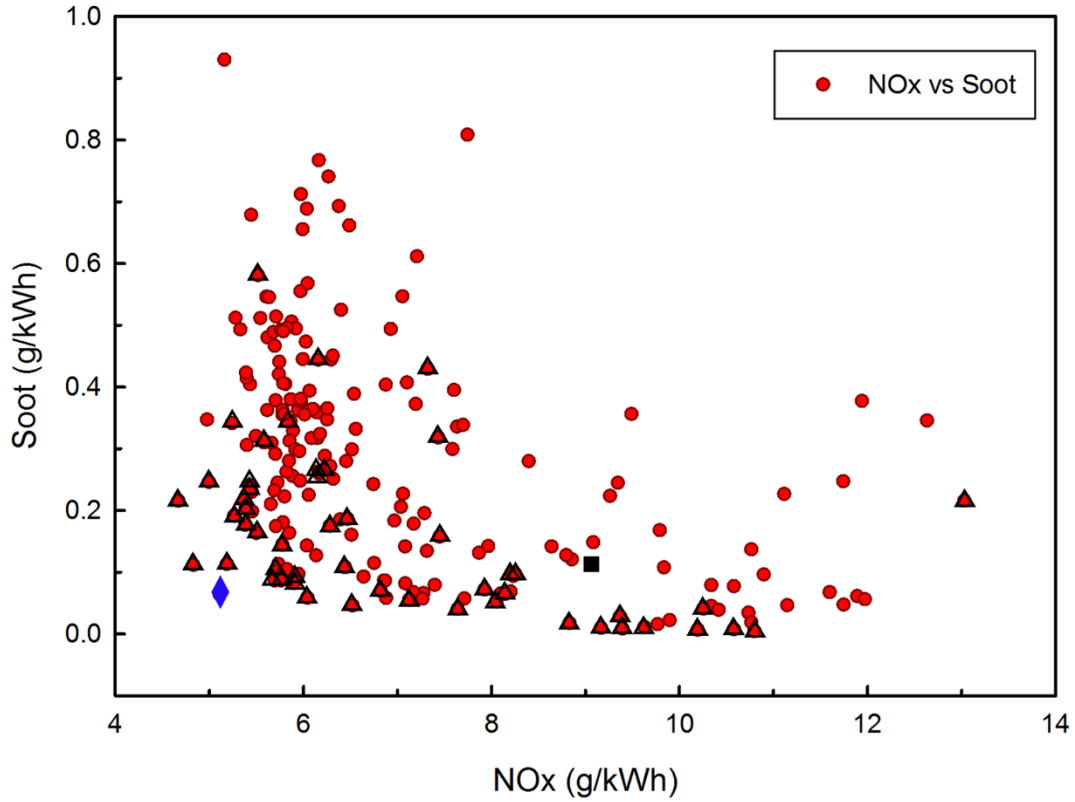

284

285 Fig. 10 NOx vs Soot of MOGA

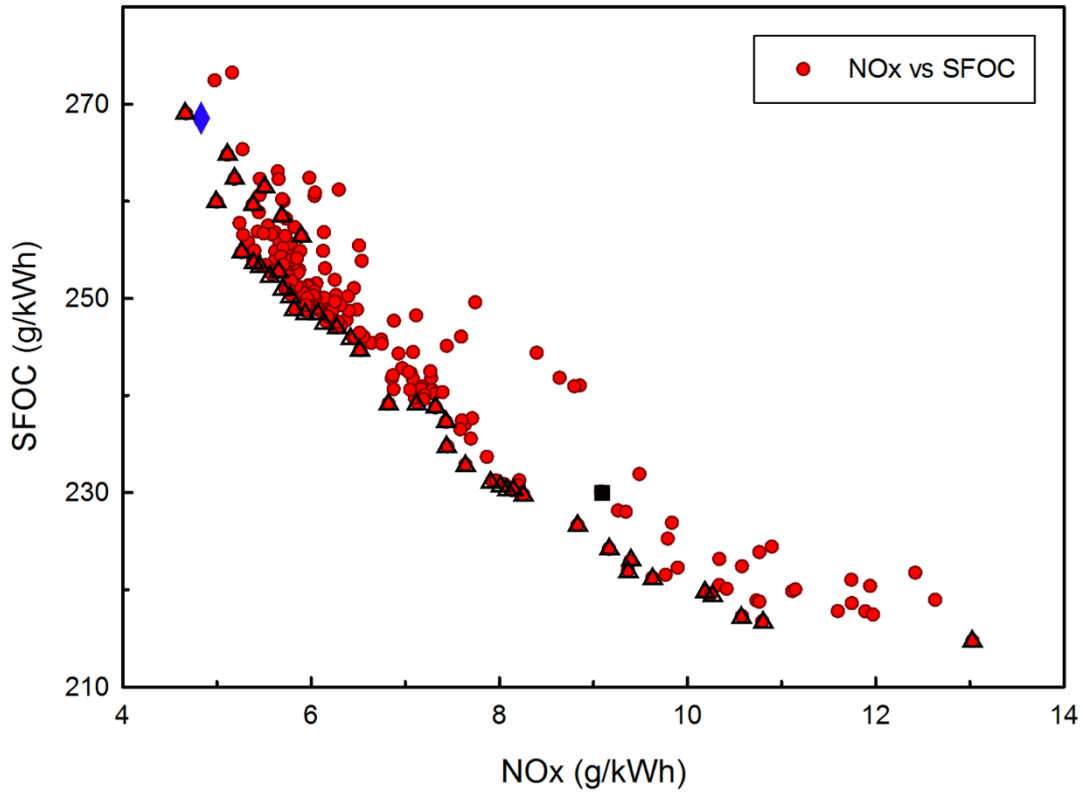

286

287 Fig. 11 NOx vs SFOC of MOGA

Table 6 Details of the objectives

Designs	NOx (g/kWh)	Soot (g/kWh)	SFOC (g/kWh)
Baseline	9.09	0.096	230
OPT_N	10.79	0.005	221
OPT_M	5.11	0.064	264

4.3 Sub-objective comparison

Table 7 gives the details information about the best sub-objectives of NLPQL algorithm and MOGA. The light blue background in Table 7 brings out the minimum values that each best sub-objective case can achieve. Comparing to the baseline design, regardless of the huge reduction achieved by both algorithms, here more attentions are paid to the differences between these best sub-objectives obtained by NLPQL algorithm and MOGA. As it can be seen that NOx_M shows an overwhelming lower sub-objectives than that of NLPQL algorithm. The sub-objectives of best soot designs were approximately the same. The best SFOC cases of both algorithms were reported to have approximate the same SFOC and extreme heavy NOx emissions. However, a slightly lower soot emissions were gained by SFOC_M.

Table 7 Best sub-objective comparisons of NLPQL algorithm and MOGA

Designs	NOx (g/kWh)	Soot (g/kWh)	SFOC (g/kWh)
Baseline	9.09	0.096	230
NOx_N	5.08	0.5213	273
NOx_M	4.67	0.2153	269
Soot_N	10.79	0.0050	221
Soot_M	10.78	0.0044	217

SFOC_N	16.59	0.2372	210
SFOC_M	19.17	0.1416	208

304

305 4.4 Design parameter comparison

306 Table 8 shows the design parameters of the best sub-objective designs. Some commonalities
307 were apparent that low NOx designs prefer late injection and small swirl, while low SFOC
308 designs are relating to early injection, large swirl and large nozzle protrusion length. Detailed
309 explanations will be given later.

310

311 Table 8 Design parameters comparisons of designs with best sub-objectives

Designs	SOI (CA)	Swirl ratio	Spray angle (deg)	Nozzle protrusion length (mm)	Bowl diameter (mm)	Centre crown height (mm)	Toroidal radius (mm)
Baseline	710.0	1.0	143.0	2.5	120	6.0	20.0
NOx_N	717.9	0.5	154.2	1.1	132	8.9	18.4
NOx_M	719.0	0.6	143.8	3.2	109	6.5	20.3
Soot_N	713.1	1.7	145.9	2.5	120	5.7	20.1
Soot_M	704.3	1.0	145.8	2.2	123	5.5	20.3
SFOC_N	702.1	1.7	152.5	4.0	129	7.1	19.4
SFOC_M	719.3	1.9	131.7	4.0	121	7.5	20.0

312

313 Generally, MOGA is more time consuming, but gains a better design in each sub-objective and
314 offers more feasible Pareto designs. The design with better balance among sub-objectives can
315 be achieved effectively by MOGA. From the mechanism of NLPQL algorithm, a better starting
316 point is crucial to the results. If the optimal design provided by MOGA was set to the starting
317 point of NLPQL algorithm, a better optimum may turn up.

5 Combination optimisation of NLPQL algorithm and MOGA

Since the starting point provided by MOGA is supposed to be a good starting point, thus, a smaller scope for each design parameter was defined, as shown in Table 9.

Table 9 Variation ranges of parameters used for optimisation

Parameters	Code	OPT_M	Lower bound	Upper bound
Injection timing, deg	SOI	719	716	720
Swirl ratio	SR	0.6	0.3	0.9
Spray angle, deg	SA	148	141	155
Nozzle protrusion length, mm	NPL	1.4	1.0	1.8
Toroidal radius, mm	r002	21.3	20	22
Centre crown height, mm	v003	8.2	7	9
Bowl diameter, mm	2*h001	120.9	114	126

Fig. 12 reported the optimisation history of the combining optimisation process with maximum 52 runs. The best objective located at run 36 (OPT_M&N) which was indicated by the red dash line. The total runs are far less than that of MOGA. Fig. 13 and Fig. 14 show the NOx vs soot and NOx vs SFOC respectively. The blue diamond point represents the optimal design obtained by MOGA, the black circle points highlight the OPT_M&N. Obviously that OPT_M&N obtained by combining method achieved a noticeable reduction of both NOx and soot. However, it paid the price of SFOC rising. In specifically, the NOx emissions, soot emissions and SFOC of OPT_M&N are 4.53 g/kWh, 0.041g/kWh and 274 g/kWh respectively. By comparing to the OPT_M, the OPT_M&N design gained a reduction of NOx emissions and soot emissions up to 11.4% and 35.9% respectively, while got a penalty of SFOC rising by 3.6%.

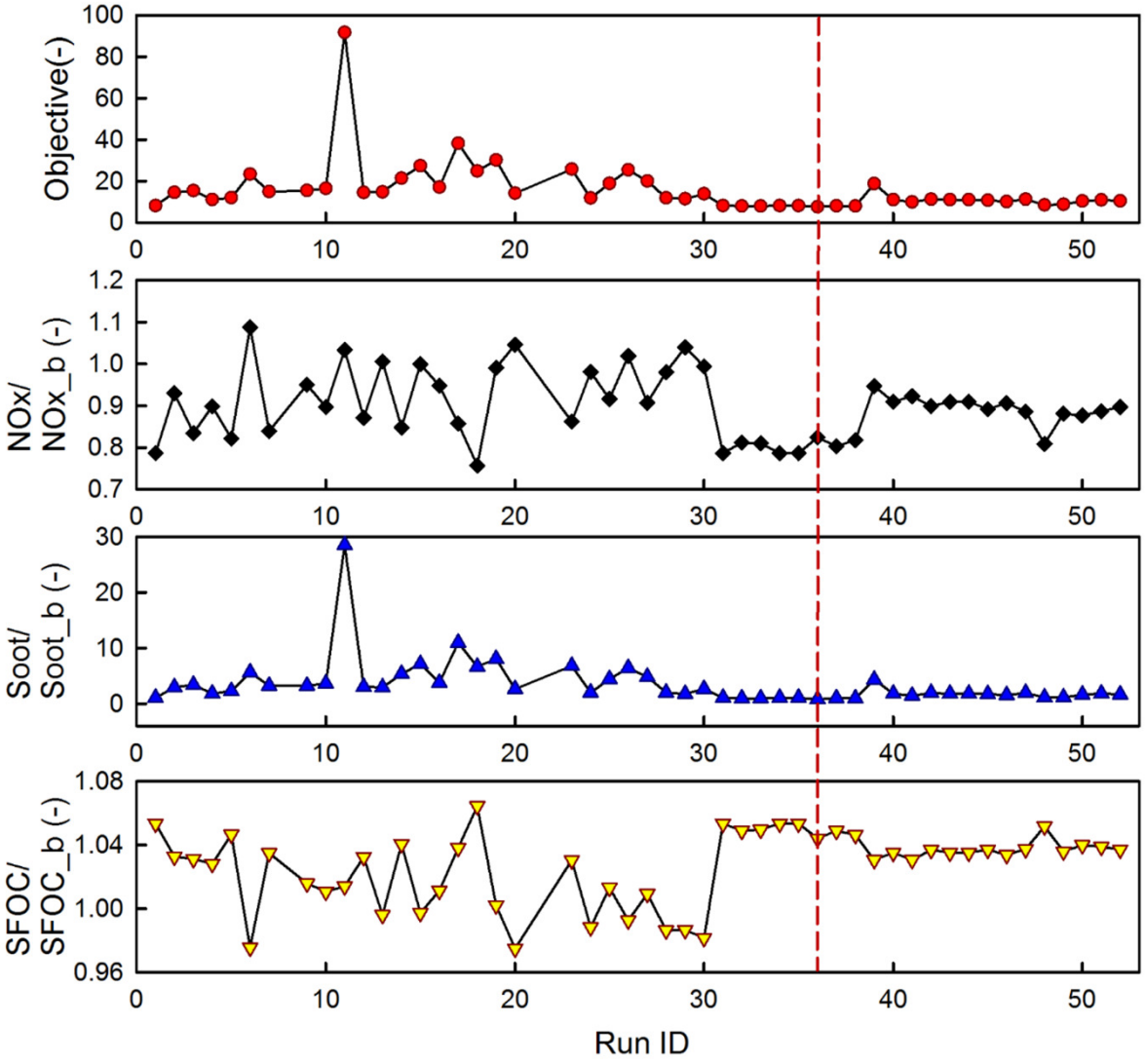

335

336 Fig. 12 Optimisation history with combining method

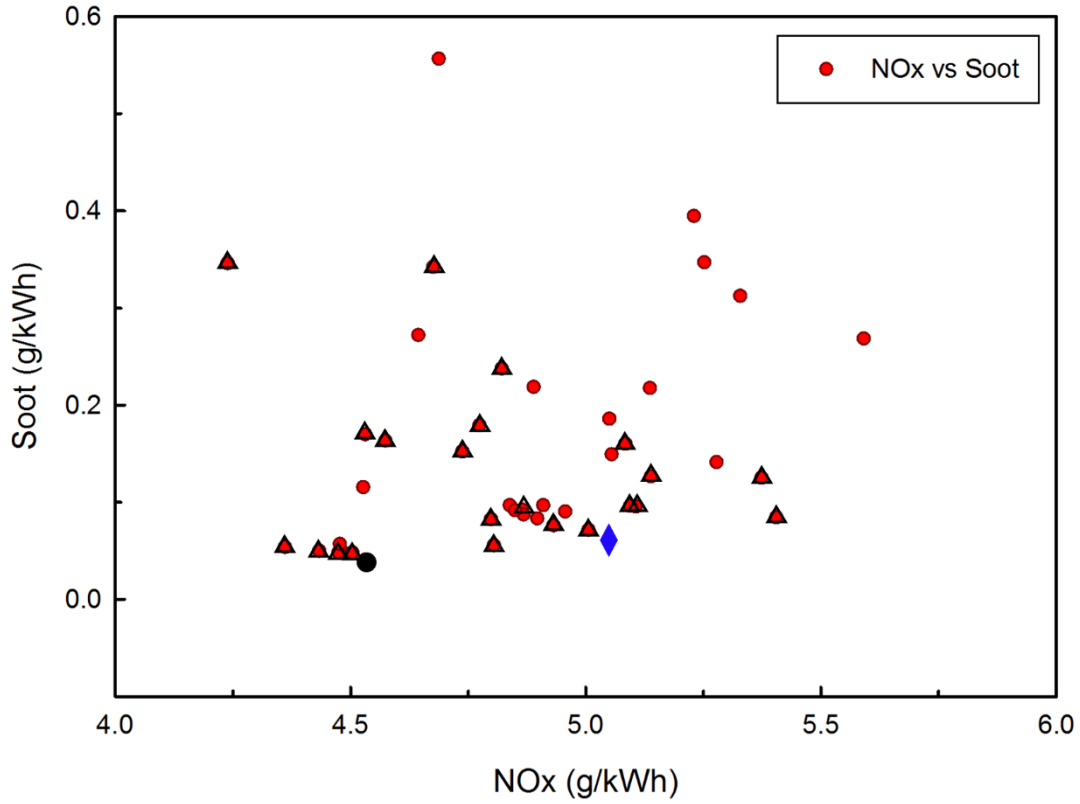

337

338 Fig. 13 NOx vs soot by combining method

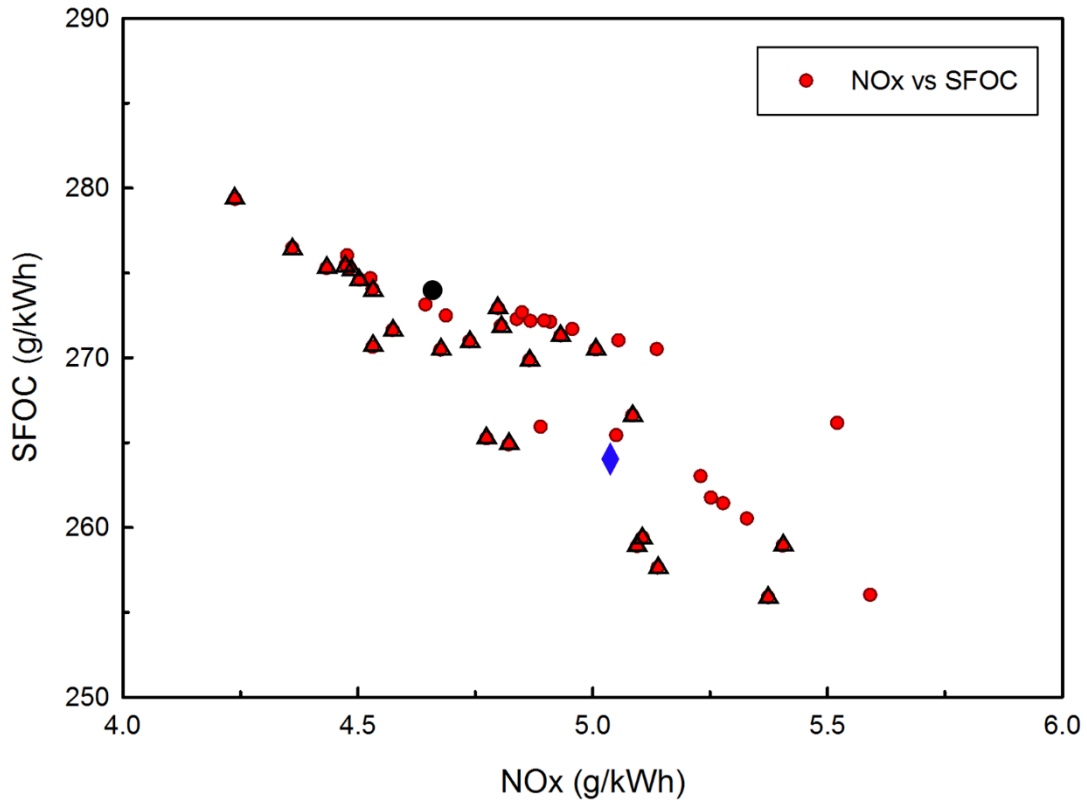

339

340 Fig. 14 NOx vs SFOC by combining method

6 Detailed combustion process of optimal designs

Table 10 reported the detailed information about the values of design parameters of the baseline design and optimal designs. Comparisons of combustion chamber shapes were shown in Fig. 15, and the combustion details were given in depth by both Fig. 16 and Fig. 17.

In Fig. 15, the baseline shape was shown as grey background, while the shapes of OPT_N, OPT_M and OPT_M&N are indicated by blue, black and red lines respectively. It can be seen that optimum designs OPT_M and OPT_M&N have larger centre crown height, larger bowl diameter or larger toroidal radius by comparing to the baseline design. The effects of these geometry features on sub-objectives are discussed in the condition of solely changing one geometry at a time. More specially, the increase of toroidal radius increases the volume of piston bowl area, which leads to a larger room for fuel-air mixing and less wall impingement of fuel with piston bowl surface. More homogenous mixing means that a better combustion was achieved, this leads to high rate of heat release and high temperature. Better combustion also helps reduce soot emissions and improves fuel economy, but high temperature encourages NOx generation. The effects of the increase of bowl diameter on sub-objectives are kind like that of the increase of toroidal radius. But too large bowl diameter results in fuel oil ejected targeting solely the bowl area of the piston to form high-density mixtures. It is not favourable for complete combustion so that encourages soot formation and leads to high SFOC. At the same time, a slightly lower temperature is achieved by comparing to that of moderate bowl diameter situation to generate less NOx emissions. Although optimal designs OPT_M and OPT_M&N both have large centre crown height, the effects of it may be far from to be noticed, due to volume increment happens in the centre of the piston and small swirl is applied.

365 Another obvious fact that optimal designs OPT_M and OPT_M&N also prefer late injection,
366 low swirl and large spray angle, as it can be seen in Table 10. Late injection offers less time
367 for fuel-air mixing, large spray angle results in some fuel adhering on the bottom of the piston
368 head and on the surface of bowl area. Because of the low swirl in the combustion chamber, two
369 separate high fuel density areas were spotted in Fig. 17. All of these lead to inadequate mixing.
370 The pent-up rate of heat release and incomplete combustion suppress the maximum
371 temperature, which is unfavourable for NOx generation. That's one of the main reasons for the
372 low NOx emissions achieved in both the MOGA and combined method. The detailed evidences
373 are provided in Fig. 16 (a), (b) and (c). Significant high soot formation rates resulting from
374 inadequate mixing were seen during combustion progress in both optimal designs of MOGA
375 and combined method. As shown Fig. 16 (d). However, high soot formation rates do not
376 necessarily mean high soot emissions in the end thanks to the high rate of soot oxidation offered
377 by high temperature in the afterburning process. The high temperature in the afterburning
378 process is the side benefit of late injection because more fuel was burned in post combustion
379 stage than the baseline and OPT_N design. Incomplete combustion occurred in these optimal
380 designs brought up high fuel consumption rate as well. High swirl ratio is beneficial for fuel-
381 air mixing, this can be proved by Fig. 17, where the injection jets were distorted to be
382 asymmetric. In 60 CA ATDC, a more homogeneous fuel distribution was seen in baseline and
383 OPT_N designs, followed by a higher rate of heat release and maximum temperature, which
384 encourages NOx formation and suppress soot generation, as shown in Fig. 16.
385
386 Table 10 Detailed design parameters of the baseline design and optimal designs

Designs	SOI (CA)	Swirl ratio	Spray angle (deg)	Nozzle protrusion length (mm)	Bowl diameter (mm)	Centre crown height (mm)	Toroidal radius (mm)

Baseline	710.0	1.0	143.0	2.5	120.0	6.0	20.0
OPT_N	713.1	1.7	145.9	2.5	119.6	5.7	20.1
OPT_M	719.0	0.6	147.9	1.7	120.9	8.2	21.3
OPT_M&N	719.6	0.3	154.5	1.0	126.0	8.9	20.2

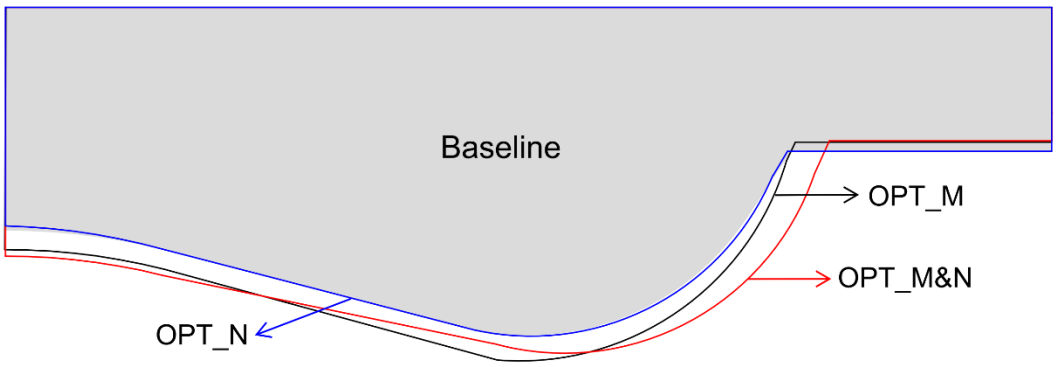

387

388 Fig. 15 Comparisons of combustion chamber shapes of the baseline design and optimal designs

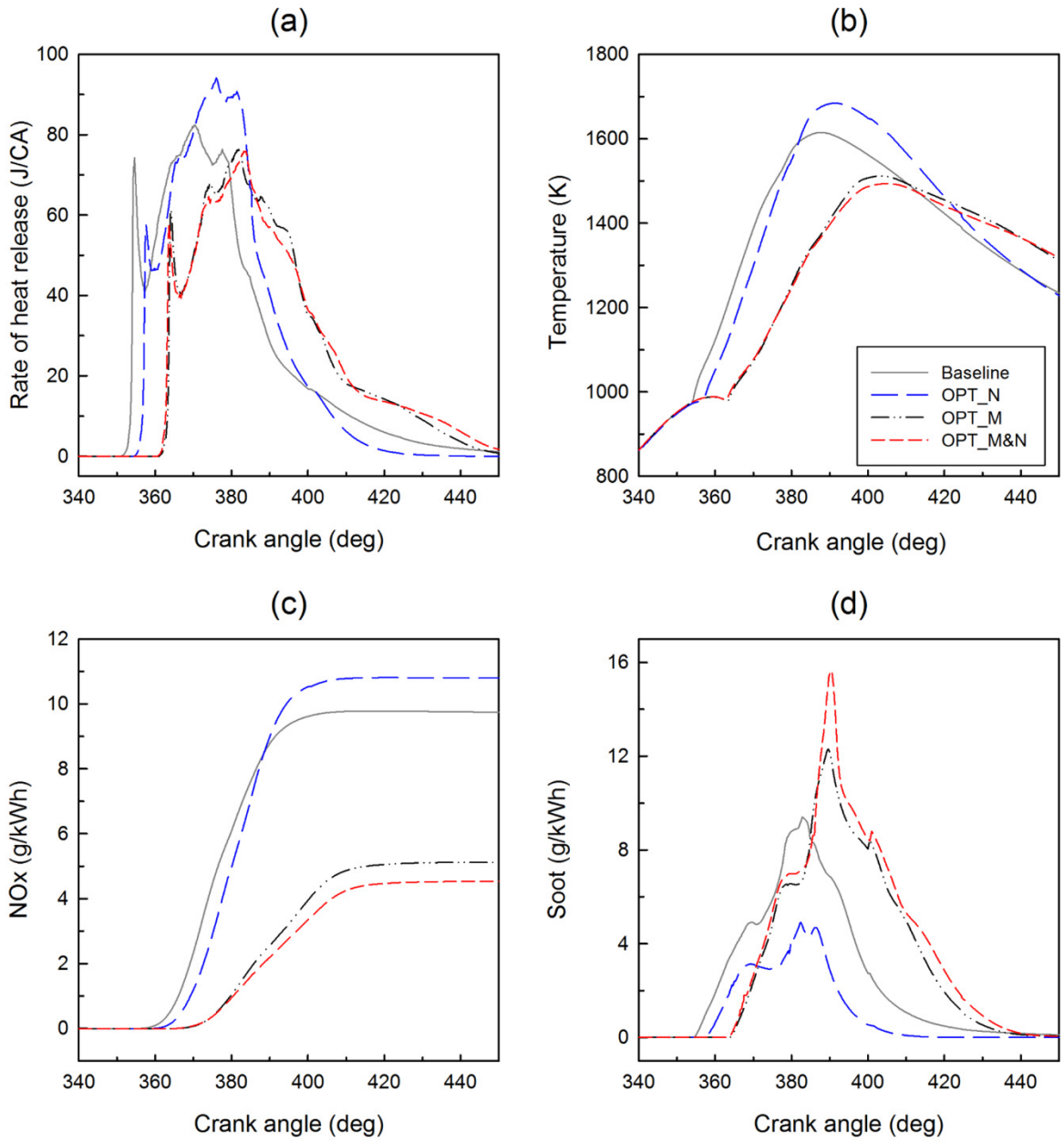

389

390 Fig. 16 Detailed comparisons of the baseline design and optimal designs

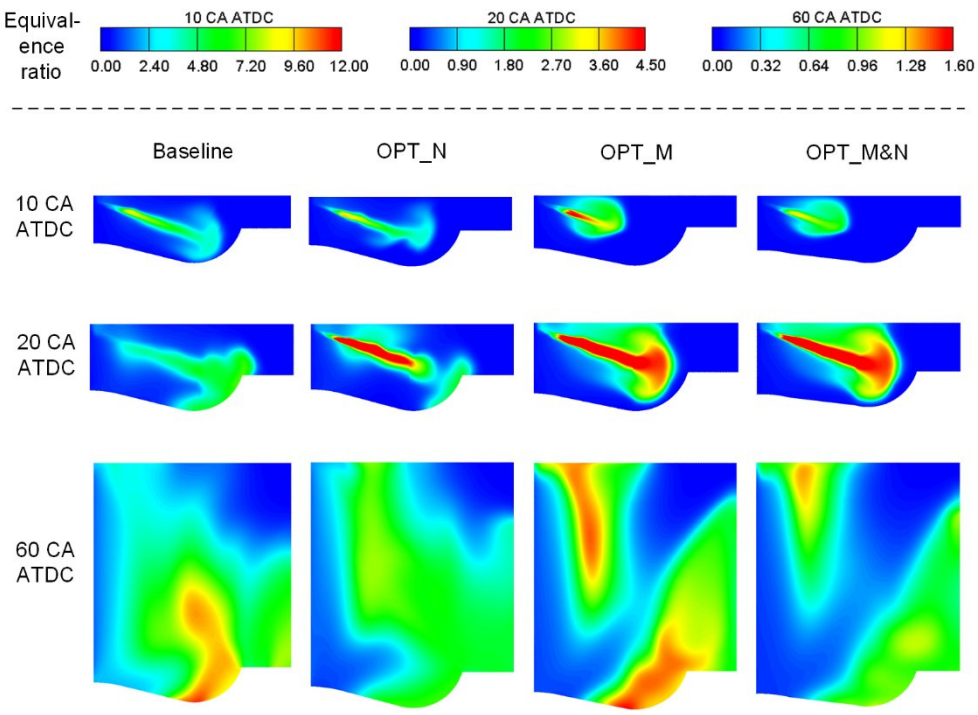

Fig. 17 CFD comparisons of fuel-air equivalence ratio of the baseline and optimal designs

7 RSM analysis

RSM was used to gain a better understanding of the influences of important design parameters on sub-objectives. Since a larger data set was obtained from MOGA, it is more suitable for RSM analysis. SS-ANOVA algorithm was used to detect the most important design parameters prior to building RSM functions. Results were shown in Fig. 18, Fig. 19 and Fig. 20. SOI has the largest effects on NOx and SFOC, followed by SR or h001. Combustion chamber parameters have a larger impact on soot than other parameters, and the bowl diameter is the most influential one. Only the parameters ranked first three were selected for generating RSM functions.

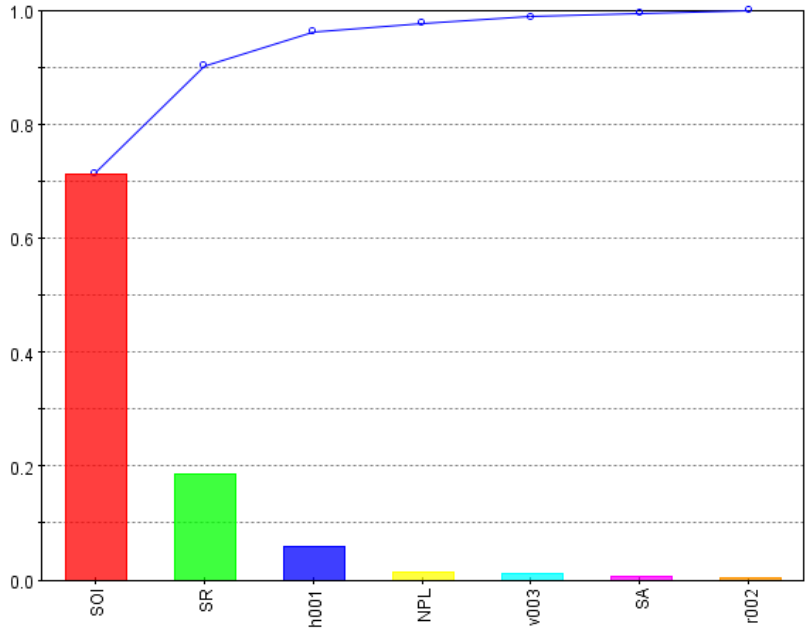

Fig. 18 Rank of effects of design parameters on NOx emissions

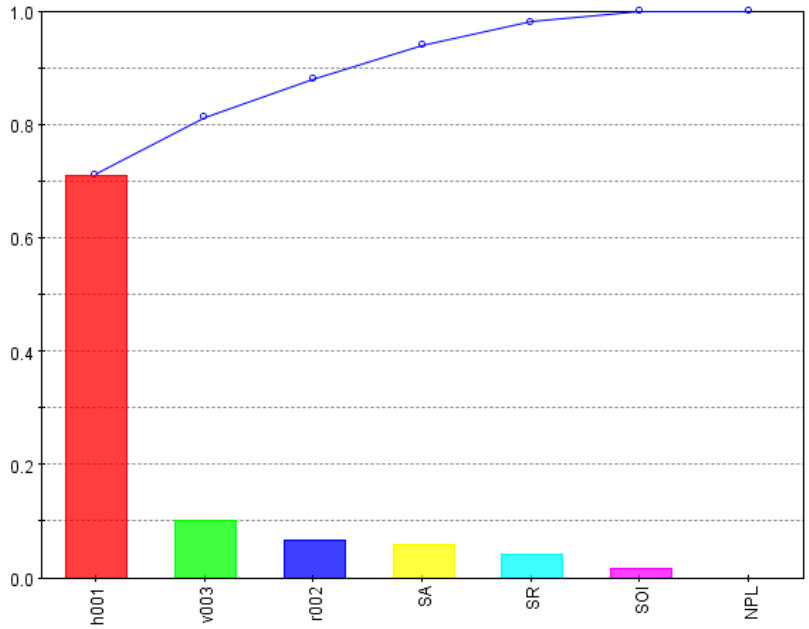

Fig. 19 Rank of effects of design parameters on soot emissions

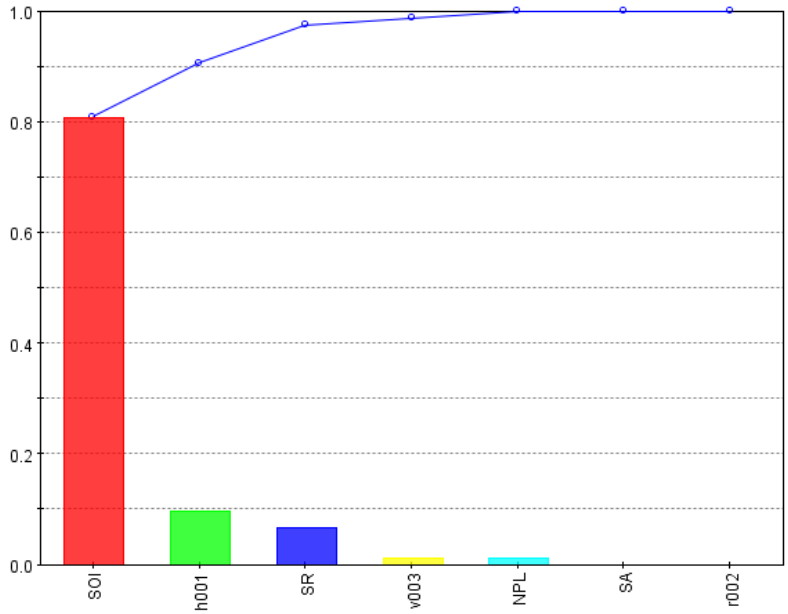

406

407 Fig. 20 Rank of effects of design parameters on SFOC

408

409 The RSM contour charts were generated by these important parameters on sub-objectives, as
410 shown in Fig. 21. NOx, soot and SFOC were represented on the first row, second row and third
411 row respectively. From the first row, SOI has an approximate uniformly distributed impact on
412 NOx, i.e. NOx decreases with the increase of SOI. SR has a significant influence when it is
413 larger than 2, which greatly deteriorates NOx emissions. SFOC increases with the increase of
414 SOI, which is also the most influential factor. Reasons were already discussed in previous
415 section. The second row indicates that a large amount of soot would be generated in the
416 condition of h001 larger than 62mm and v003 lower than 6.8mm.

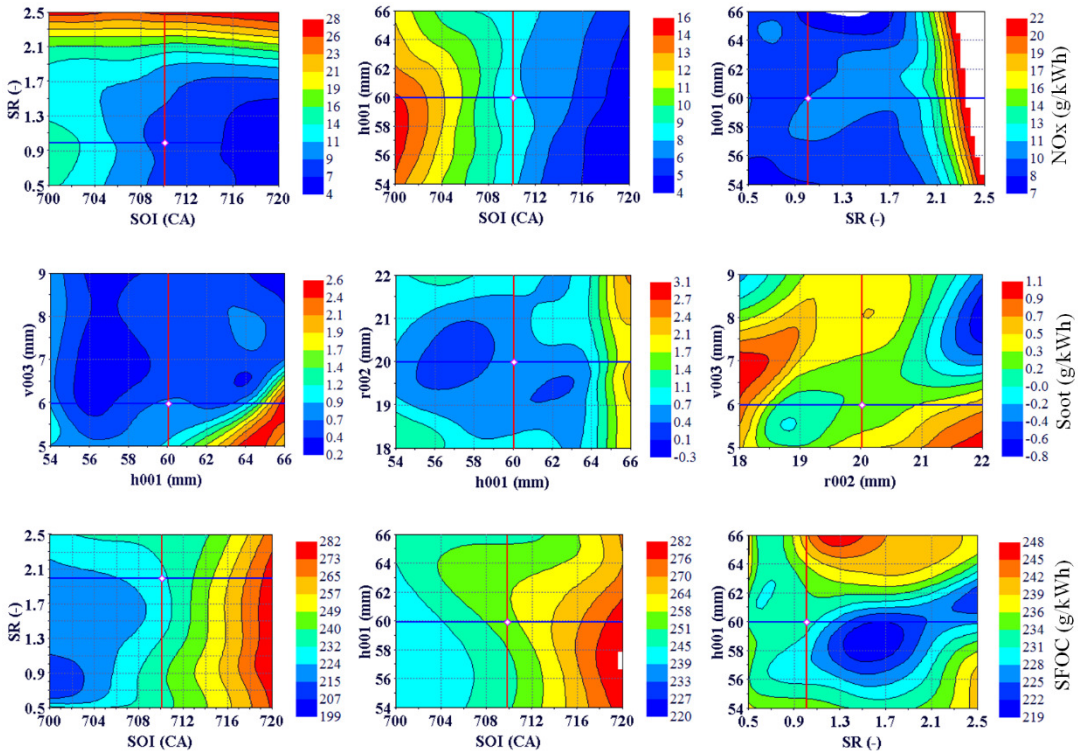

Fig. 21 RSM contour maps

8 Conclusions

Seven engine parameters were investigated by using NLPQL algorithm and MOGA separately and together. Comparisons were made on both objectives, sub-objectives, design parameters and detailed combustion processes. Then, RSM was used to gain a better understanding of design parameters on sub-objectives. The main conclusions are list as follows.

(1) NLPQL algorithm approach optimal designs faster than MOGA with fewer runs, however, the weights of merit function should be selected carefully;

(2) NLPQL algorithm is not that effective when it is introduced for the optimisation task with seven engine parameters.

(3) MOGA is more time consuming but offers broader and finer solutions. Hence, more Pareto designs are provided and a better design is obtained in each sub-objective than that of NLPQL algorithm.

(4) If a good starting point was given by MOGA, NLPQL algorithm is an effective way for offering a better optimal design.

(5) SOI has the dominant and clearly opposite effects on NOx and SFOC.

(6) NOx and soot can be reduced greatly at the same time by adopting late injection, low swirl and large spray angle together, but fuel economy was sacrificed.

(7) Combustion chamber geometries are influential to soot emissions.

Acknowledgment

Authors are grateful to the Department of Naval Architecture and Marine Engineering of University of Strathclyde for the calculation support on the project. We also appreciate the Wuhan University of Technology for providing experimental facilities and test data.

Funding: This work was supported by the project ‘An Investigation into the Characteristics of High-pressure Common Rail Injection System’ from Lloyds Register of Shipping of UK and the project ‘Key Technologies Research of Intelligent Control System for Marine Medium-speed Diesel Engine’ from Ministry of Industry and Information Technology of the People's Republic of China.

Reference

[1] Taghavifar H, Khalilarya S, Jafarmadar S. Engine structure modifications effect on the flow behavior, combustion, and performance characteristics of DI diesel engine. Energy Conversion and Management 2014; 85: 20-32.

[2] Park S. Optimisation of combustion chamber geometry and engine operating conditions for compression ignition engines fueled with dimethyl ether. Fuel 2012; 61-71.

[3] Mobasheri R and Peng Z, Analysis of the effect of re-entrant combustion chamber geometry on combustion process and emission formation in a HSDI diesel engine. SAE International; 2012-01-0144.

[4] Genzale CL, Reitz RD, Wickman DD. A computational investigation into the effects of spray targeting, bowl geometry and swirl ratio for low-temperature combustion in a heavy-duty diesel engine. SAE Technical Paper Series; 2007-01-0119.

[5] Genzale CL, Reitz RD, Mark PB. Effects of piston bowl geometry on mixture development and late-injection low-temperature combustion in a heavy-duty diesel engine. SAE Int. J. Engines; 2008-01-1330.

[6] Ge HW, Shi Y, Reitz RD. Optimisation of a HSDI diesel engine for passenger cars using a multi-objective genetic algorithm and multi-dimensional modelling. SAE Int. J. Engines; 2009-01-0715.

[7] Shi Y and Reitz RD. Optimisation study of the effects of bowl geometry, spray targeting, and swirl ratio for a heavy-duty diesel engine operated at low and high load. Int. J. Engine Res. 2008; 9: 325-346.

[8] Taghavifar H, Jafarmadar S, Taghavifar H**,** Navid A. Application of DoE evaluation to introduce the optimum injection strategy-chamber geometry of diesel engine using surrogate epsilon. Applied Thermal Engineering 2016; 106: 56-66.

[9] Jeong S, Obayashi S, Minemura Y. Application of hybrid evolutionary algorithms to low exhaust emission diesel engine design. Eng Optimization 2008; 40(1):1-16.

[10] Chen Y and Lv L. The multi-objective optimisation of combustion chamber of DI diesel engine by NLPQL algorithm. Applied Thermal Engineering 2014; 1332-1339.

[11] Shi Y and Reitz RD. Assessment of optimisation methodologies to study the effects of bowl geometry, spray targeting and swirl ratio for a heavy-duty diesel engine operated at high-load. SAE Int. J. Engines; 2008-01-0949.

[12] Navid A, Khalilarya S, Taghvifar H. Comparing multi-objective non-evolutionary NLPQL and evolutionary genetic algorithm optimisation of a DI diesel engine: DoE estimation and creating surrogate model. Energy Conversion and Management 2016; 126: 385-399.

[13] User Guide of Design of Experiments and Optimisation, Version 2013. Austria: AVL LIST GmbH; 2013.

[14] Ali OM, Mamat R, Najafi G, Yusaf T, Ardebili SMS. Optimization of biodiesel-diesel blended fuel properties and engine performance with ether additive using statistical analysis and response surface methods. Energies 2015; 8(12): 14136-14150.

[15] Taghavifar H, Taghavifar H, Mardani A and Mohebbi A. Modeling the impact of in-cylinder combustion parameters of DI engines on soot and NOx emissions at rated EGR levels using ANN approach. Energy Conversion and Management 2014; 87: 1-9.

[16] Taghavifar H, Taghavifar H, Mardani A, Mohebbi A, Khalilarya S and Jafarmadar S. On the modeling of convective heat transfer coefficient of hydrogen fueled diesel engine as affected by combustion parameters using a coupled numerical-artificial neural network approach. International journal of hydrogen energy 2015; 40(12): 4370-4381.

[17] Taghavifar H, Taghavifar H, Mardani A, Mohebbi A. and Khalilarya S. A numerical investigation on the wall heat flux in a DI diesel engine fueled with n-heptane using a coupled CFD and ANN approach. Fuel 2015; 140: 227-236.

[18] Abbasi B and Mahlooji H. Improving response surface methodology by using artificial neural network and simulated annealing. Expert Systems with Applications 2012; 39: 3461-3468.

[19] Whiteman JK and Gueguim Kana EB. Comparative assessment of the artificial neural network and response surface modelling efficiencies for biohydrogen production on sugar cane molasses. Bioenerg. Res. 2014; 7: 29-305.

[20] Tosun E, Aydin K, Bilgili M. Comparison of linear regression and artificial neural network model of a diesel engine fueled with biodiesel-alcohol mixtures. Alexandria Engineering Journal 2016; 1-9.

[21] Schittkowski K. NLPQL: A fortran subroutine solving constrained nonlinear programming problems. Annals of operations research 1985; 5(6): 485-500.

[22] Senecal Pk, Pomraning E, Richards KJ. Multi-mode genetic algorithm optimisation of combustion chamber geometry for low emissions. SAE 2002 World Congress; 2002-01-0958.

[23] Abdullah K, David WC, Alice ES. Multi-objective optimisation using genetic algorithms: A tutorial. Reliability Engineering and System Safety 2006; 91: 992-1007.

[24] Nikoskinen T. From neural networks to deep neural networks. Aalto University School of Science 2015.

[25] Levenberg K, A method for the solution of certain problems in least squares, Quarterly of Applied Mathematics 1994; 5: 164-168.

[26] Marquardt D, An algorithm for least-squares estimation of nonlinear parameters, SIAM Journal on Applied Mathematics 1963; 11(2): 431-441.

[27] Hanjalic K, Popovac M, Hadziabdic M. A robust near-wall elliptic relaxation eddy-viscosity turbulence model for CFD. International Journal of Heat and Fluid Flow 2004; 25: 1047-1051.

[28] Popovac M and Hanjalic K. Compound wall treatment for RANS computation of complex turbulent flows and heat transfer. Flow Turbulence and Combustion 2007; 78: 177-202.

[29] Issa RI. Solution of the implicit discretised fluid flow equations by operator splitting. Journal of Computational Physics 1985; 62: 45-60.

[30] Emans M. AMG for Linear Systems in Engine Flow Simulations. PPAM 2009, Part II, LNCS 6068; 350-359.

[31] Dukowicz JK. Quasi-steady droplet change in the presence of convection. Los Alamos Scientific Laboratory. LA7997-MS.

[32] Liu A, Mather D, Reitz RD. Modelling the effects of drop drag and breakup on fuel sprays, SAE Technical Paper 1993; doi: 10. 4271/930072.

[33] Reitz RD, Modelling atomization processes in high-pressure vaporizing sprays, Atomization and Spray Technology 1987; 3: 309-337.

[34] Naber JD and Reitz RD. Modelling engine spray/wall impingement. SAE 1988; 880107.

[35] Cabrera E, Gonzalez JE., Heat flux correlation for spray cooling in the nucleate boiling regime. Exp. Heat Transfer 2003; 16: 19-44.

[36] Spalding DB. Mixing and chemical reaction in steady confined turbulent flames. Symposium (International) on Combustion 1971; 13(1): 649-657.

[37] Magnussen BF and Hjertager BH. On mathematical modelling of turbulent combustion with special emphasis on soot formation and combustion. Symposium (International) on Combustion 1997; 16(1): 719-729.

[38] Zeldovich YA, Frank-Kamenetskii D, Sadovnikov P. The oxidation of nitrogen in combustion and explosions. Publishing House of the Academy of Sciences of USSR 1947.

[39] Wang H and Frenklach M. A detailed kinetic modelling study of aromatics formation, growth and oxidation in laminar premixed ethylene and acetylene flames. Combustion and Flame 1997; 110: 173-221.

[40] Apple J, Bockhorn H, Frenklach M. Kinetic modelling of soot formation with detailed chemistry and physics: laminar premixed flames of C2 hydrocarbons. Combustion and Flame 2000; 121: 122-136.

[41] Balthasar M and Frenklach M. Detailed kinetic modelling of soot aggregate formation in laminar premixed flames. Combustion and Flame 2005; 140: 130-145.

[42] Light diesel oil. http://www.optionengg.net/ldo.htm.

[43] Abraham J, What is adequate resolution in numerical computations of transient jets? SAE Technical Paper, 1997-00-51.